Crystal Structure of Vat(D): An Acetyltransferase That Inactivates Streptogramin Group A Antibiotics[†,‡]

Michele Sugantino and Steven L. Roderick*

Department of Biochemistry, Albert Einstein College of Medicine, 1300 Morris Park Avenue, Bronx, New York 10461

Received October 30, 2001; Revised Manuscript Received December 14, 2001

ABSTRACT: The streptogramin class of antibiotics act to inhibit bacterial protein synthesis, and their semisynthetic derivatives, such as dalfopristin−quinupristin (Synercid), are used to treat serious or life-threatening infections due to multiply antibiotic resistant bacteria. Acquired resistance of the nosocomial pathogen *Enterococcus faecium* to the group A component of natural and semisynthetic streptogramin mixtures is a prerequisite for the streptogramin resistance phenotype and is mediated by a streptogramin acetyltransferase. The crystal structure of Vat(D), a streptogramin acetyltransferase from a human urinary isolate of *E. faecium*, has been determined as an apoenzyme and in complex with either acetyl-CoA or virginiamycin M_1 and CoA. These structures illustrate the location and arrangement of residues at the active site, and point to His 82 as a residue that may function as a general base. The structural similarity of Vat(D) to the xenobiotic acetyltransferase from *Pseudomonas aeruginosa* indicates similarities in the catalytic mechanism for these enzymes as well as several shared and distinctive antibiotic binding interactions between these enzymes and their respective substrates. These results reveal the molecular basis for a reaction by which Gram-positive cocci acquire resistance to a last resort antibiotic.

Antibiotics of the streptogramin class are natural products produced predominantly by members of the genus *Streptomyces* as a complex of structurally unrelated group A and group B compounds (*4*). Group A compounds are polyunsaturated macrolactones typified by virginiamycin M_1 (pristinamycin II_A; Figure 1). Group B components are cyclic hexadepsipeptides and include virginiamycin S_1 and pristinamycin I_A. Group A and group B compounds are produced jointly in nature and bind synergistically to different target sites on the 50S ribosomal subunit to inhibit bacterial protein elongation. Although the A and B compounds are individually bacteriostatic to sensitive strains, the mechanism of streptogramin inhibition is synergistic and is frequently bactericidal.

Although naturally produced streptogramins have been used orally and topically to treat human bacterial infections (e.g., virginiamycin and pristinamycin), the insolubility of these preparations has limited their intravenous use. Recently, Synercid (Rhône-Poulenc Rorer), a water-soluble and injectable semisynthetic streptogramin composed of a 70:30 mixture of dalfopristin (group A) and quinupristin (group B) components, has been approved as a last resort treatment for severe infections due to a variety of bacteria, including methicillin-resistant *Staphylococcus aureus* and multidrug or vancomycin-resistant *Enterococcus faecium*.

Genes encoding resistance factors to streptogramin antibiotics and their metabolites, including the quinupristin−dalfopristin complex, have been identified, and their mechanisms of resistance have been determined (*5*−*11*). Resistance to the group B components of streptogramin mixtures is

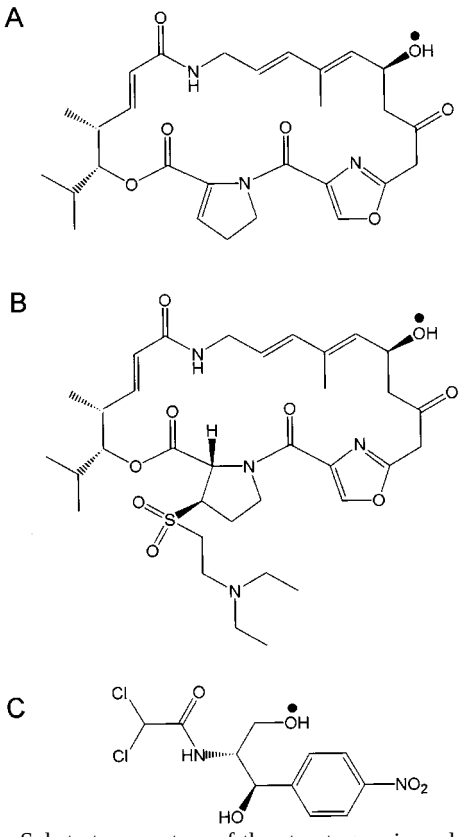

FIGURE 1: Substrate acceptors of the streptogramin and chloramphenicol hexapeptide acetyltransferases: (A) virginiamycin M_1, (B) dalfopristin, the group A semisynthetic component of Synercid, and (C) chloramphenicol. The positions of the modified hydroxyl groups are indicated (●).

[†] This work was supported by Grant AI42154.

[‡] The coordinates have been deposited in the Protein Data Bank (entries 1KHR, 1KK4, 1KK5, and 1KK6).

* To whom correspondence should be addressed. Phone: (718) 430-2784. Fax: (718) 430-8565. E-mail: roderick@aecom.yu.edu.

10.1021/bi011991b CCC: $22.00
Published on Web 01/25/2002

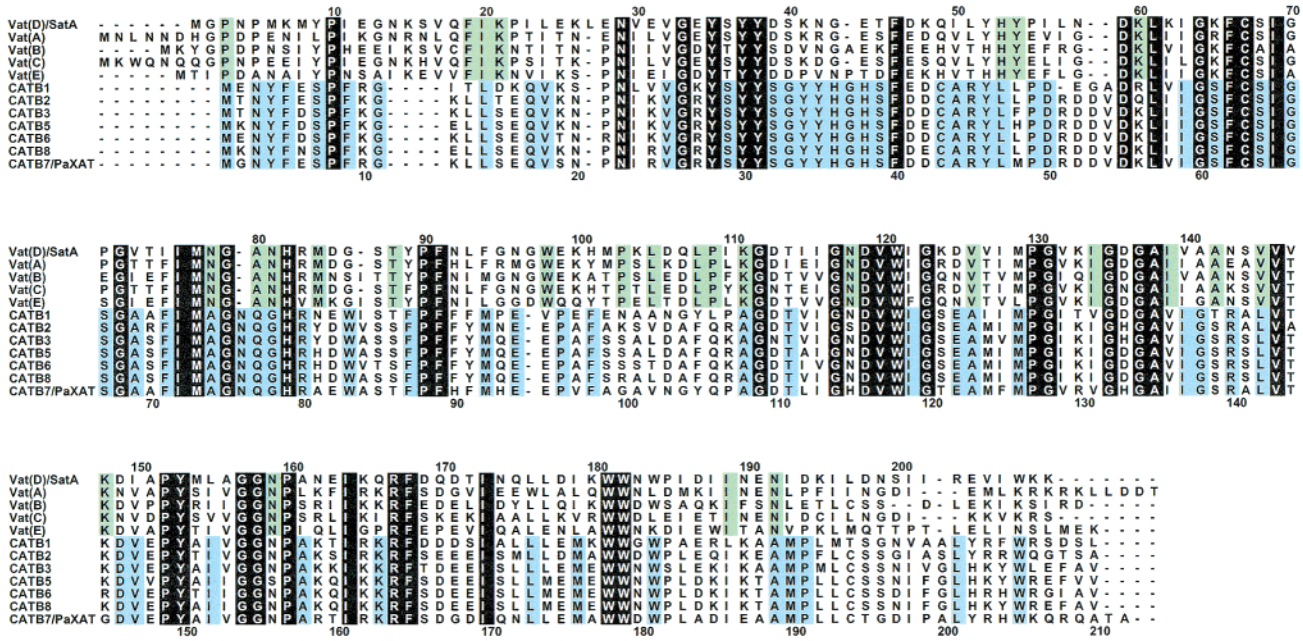

FIGURE 2: Amino acid sequence alignment of Vat and CATB enzymes.[2] Conserved residues among the Vat and CATB sequences are shaded green and blue, respectively. The residues that are conserved in all sequences are reverse shaded. The numbering scheme above the alignment refers to the Vat(D)/SatA sequence. The numbering scheme below the alignment refers to the CATB7/PaXAT sequence. The alignment and figure were produced with Jalview and Alscript (*34*).

mediated by 23S rRNA target methylation by members of the *erm* gene class to produce the MLS_B[1] resistance phenotype (*12*) or by linearization of the hexadepsipeptide ring by specific lyases (*11*). Resistance to the group A component is mediated by drug efflux in members of the genus *Staphylococcus* and more generally by CoA-dependent O-acetylation of the hydroxyl group of these compounds (*5*). Molecular analysis of resistance plasmids from Gram-positive cocci indicates that marked resistance to streptogramins requires the presence of a *vat* gene from a family encoding group A streptogramin acetyltransferases (Figure 2) (*1*, *10*).

Vat enzymes are members of the hexapeptide repeat family of acyltransferases that contain tandem repeated imperfect copies of a six-residue amino acid sequence repeat motif termed a hexapeptide repeat (*13*, *14*). Crystal structure analysis of several hexapeptide acyltransferases demonstrates that the hexapeptide repeat motif directs folding of a characteristic coiled LβH domain in these trimeric enzymes (*15*−*22*). The acyl donors are acetyl- or succinyl-CoA thioesters or fatty acyl thioesters of the acyl carrier protein. A diverse range of acceptors bearing free hydroxyl or amino groups are recognized, including antibiotics and intermediates involved in cell wall biosynthesis and amino acid metabolism.

Among the members of the hexapeptide acyltransferase family of enzymes are those that are capable of acetylating Clm or the group A component of streptogramins (*23*). The enzymes that acetylate Clm have been categorized as CATB (*3*) enzymes to distinguish them from the unrelated classical CATA or CAT_{III} chloramphenicol acetyltransferases (*24*). Given that the CATB enzymes confer only moderate resistance to Clm in most organisms and generally display 12−75-fold greater K_m values for Clm than for the CAT_{III} (CATA) chloramphenicol acetyltransferases (*3*, *23*), it has been suggested that the natural substrate for these enzymes is not Clm (*23*). The hexapeptide acyltransferases that acetylate the group A component of streptogramins are generally 46−70% identical in amino acid sequence and exhibit 34−43% pairwise amino acid sequence identity to the CATB Clm acyltransferases (Figure 2). Collectively, these enzymes have also been termed xenobiotic acetyltransferases (XATs) (*23*).

The crystal structure of a chromosomal xenobiotic acetyltransferase from *Pseudomonas aeruginosa* PA103 (PaXAT, CATB7) capable of acetylating Clm has been determined in complex with Clm and desulfo-CoA (*18*), although to date structural characterization of any enzyme that covalently inactivates streptogramins has not been reported. Here, we report the crystal structure of Vat(D),[3] a streptogramin acetyltransferase from the human urinary isolate *E. faecium* BM4145 that inactivates virginiamycin M_1, a group A component of streptogramin, as well as the group A (dalfopristin) component of Synercid (*5*). These studies describe the overall fold and active site architecture of the enzyme and provide a basis for understanding the binding

[1] Abbreviations: Clm, chloramphenicol; CoA, coenzyme A; LβH, left-handed parallel β-helix; MLS_B, macrolide−lincosamide−streptogramin$_B$; PaXAT, *Pseudomonas aeruginosa* xenobiotic acetyltransferase (identical to CATB7); rms, root-mean-square.

[2] The source and amino acid sequence accession codes for Vat (*1*) and CATB (*2*, *3*) enzymes: Vat(D)/SatA (*E. faecium* BM4145, AAA24783), Vat(A) (*S. aureus* pIP680, AAA26683), Vat(B) (*S. aureus* pIP1633, AAA86871), Vat(C) (*Staphylococcus conhii* pIP1714, AAC61671), Vat(E) (*E. faecium* UW1965, AAD44719), CATB1 (*Agrobacterium tumefaciens* C58, AAA22081), CATB2 (*Es. coli* W677/Tn2424, AAC14737), CATB3 (*Enterococcus aerogenes* pBWH301, AAA90938), CATB5 (*Morganella morganii* Tn840, CAA57832), CATB6 (*P. aeruginosa* In101, CAA11473), CATB8 (*Klebsiella pneumoniae* pKB42, AAF61918), and CATB7/PaXAT (*P. aeruginosa* PA101, AAD02068).

[3] Vat(D) is also termed SatA (*1*).

Table 1: Data Measurement and Structure Refinement Statistics[a]

	apoenzyme	apoenzyme	acetyl-CoA	CoA−virginiamycin
crystal form	I	II	II	II
no. of unique subunits	3	6	6	6
data measurement				
resolution (Å)	2.5	2.7	2.7	2.8
no. of observed reflections	106003	214923	152101	135079
no. of unique reflections	26649	43352	42109	37772
redundancy	4.0	5.2	3.6	3.6
R_{merge} (%)	8.2 (26.9)	6.8 (19.2)	7.6 (20.0)	8.9 (29.6)
completeness (%)	99.0 (96.4)	99.7 (83.1)	94.0 (84.4)	93.5 (91.9)
no. of atoms				
protein	4852	9706	9720	9684
substrate	−	−	306	288/114
water	141	162	151	112
rms deviation from ideality				
bond lengths (Å)	0.010	0.010	0.010	0.009
bond angles (deg)	1.5	1.4	1.6	1.5
average thermal factor (Å^2)				
protein atoms	23.8	23.0	23.1	20.4
substrate atoms	−	−	49.7	35.8/32.1
solvent atoms	36.0	37.8	40.4	33.1
R_{factor}/R_{free} (%)	20.6/28.0 (27.9/30.7)	19.2/25.4 (25.1/31.3)	19.1/26.0 (25.7/30.7)	18.9/25.1 (24.8/32.1)

[a] Data measurement and structure refinement statistics for the Vat(D) structures. R_{merge} (%) $= \sum|I_i - \langle I\rangle|/\sum|I_i| \times 100$, where I_i is an individual intensity observation, $\langle I\rangle$ is the mean intensity for that reflection, and the summation is over all reflections. Numbers in parentheses refer to the highest-resolution shell: apo form I, 2.60−2.50 Å; apo form II, 2.80−2.70 Å; acetyl-CoA, 2.80−2.70 Å; and CoA−virginiamycin M_1, 2.90−2.80 Å. Completeness is the ratio of the number of observed unique reflections to the total number of theoretically possible reflections × 100. R_{factor} (%) $= \sum|F_o - F_c|/\sum|F_o| \times 100$ for all available data. R_{free} (%) $= \sum|F_o - F_c|/\sum|F_o| \times 100$ for a 5% subset of X-ray diffraction data omitted from refinement calculations.

specificity of Vat(D) for its cofactor and group A compound substrates as well as the catalytic activity of an important resistance determinant to the streptogramin class of antibiotics. Comparison of the structures of Vat(D) with PaXAT reveals the means by which these hexapeptide acyltransferases inactivate structurally dissimilar antibiotics in the context of a structurally similar polypeptide chain fold.

EXPERIMENTAL PROCEDURES

Enzymatic Assay of PaXAT and Vat(D). Vat(D) activity was assayed using a Uvikon 9310 spectrophotometer (Kontron) equipped with thermospacers and connected to a constant-temperature circulating water bath at 25 °C. The standard assay mixture contained 50 mM K_2HPO_4 (pH 7.5) and 3 mM 5,5′-dithiobis(2-nitrobenzoic acid), and the reaction was initiated with the addition of 5 μL of 11 μg/mL Vat(D) and monitored at 410 nm. The apparent K_m and V_{max} were determined by holding the concentration of virginiamycin M_1 constant at 500 μM and varying the acetyl-CoA concentration (from 100 μM to 1 mM) or keeping the acetyl-CoA concentration constant at 1 mM and varying the concentration of virginiamycin M_1 (from 8 to 250 μM). Assays of Vat(D) activity using Clm as the substrate were carried out with Clm concentrations of up to 0.1 M. Kinetic parameters were calculated with the programs of Cleland (*25*).

Crystallization of Vat(D). Vat(D) was expressed and purified as previously described (*26*) and crystallized from solutions of 25−35% polyethylene glycol 400, 5−8% ethanol, and 0.2 M Tris-HCl (pH 8.0) by the hanging drop vapor diffusion method at 22 °C. Two distinct crystal forms were identified. Form I crystals were obtained only in crystallization experiments using the enzyme from the first protein preparation. These crystals belong to space group $P2_12_12_1$ (a = 68.6 Å, b = 102.6 Å, and c = 107.5 Å) and contain one trimeric molecule in the asymmetric unit. Form II crystals could be produced from all preparations and belong to orthorhombic space group $F222$ (a = 185.8 Å, b = 185.8 Å, and c = 186.5 Å) and contain two trimers per asymmetric unit.

Measurement of X-ray Data and Structure Determination. X-ray intensity data were measured at ambient temperature with a Siemens X1000 detector and Cu Kα radiation produced by a Rigaku RU-200 rotating anode X-ray generator operating at 4.0 kW. The data were processed with XDS (*27*) and scaled with XSCALE or SCALEPACK (*28*) (Table 1). The structure of the form I crystal was determined by molecular replacement using X-PLOR (*29*). The search model was a trimer of PaXAT (PDB entry 1XAT) and included predominantly residues corresponding to the structurally conserved LβH coiled domain. A single trimeric molecule was positioned and an atomic model built with O (*30*) against $2F_o - F_c$ and $F_o - F_c$ electron density maps and refined with X-PLOR, reserving 5% of the diffraction data for cross validation (*31*). Form I crystals could not be reproduced from subsequent protein preparations, and so molecular replacement was carried out with AmoRe (*32*) to determine the form II crystal structure using the newly determined form I apoenzyme coordinates as a search model. Two trimers were located in the asymmetric unit of the form II crystals, arranged with pseudo $F23$ space group symmetry.

Determination of Vat(D) Complex Structures. To determine the active-site location and conformation of bound substrates, X-ray data were measured from form II crystals that had been soaked for 7 days at room temperature in solutions containing 35% polyethylene glycol 400, 0.1 M Tris-HCl (pH 8.0), and either (1) 50 mM acetyl-CoA or (2) 50 mM CoA, 50 mM virginiamycin M_1, and 25% (v/v) dimethyl sulfoxide. The locations of CoA or acetyl-CoA were determined in each of the six active sites of the asymmetric

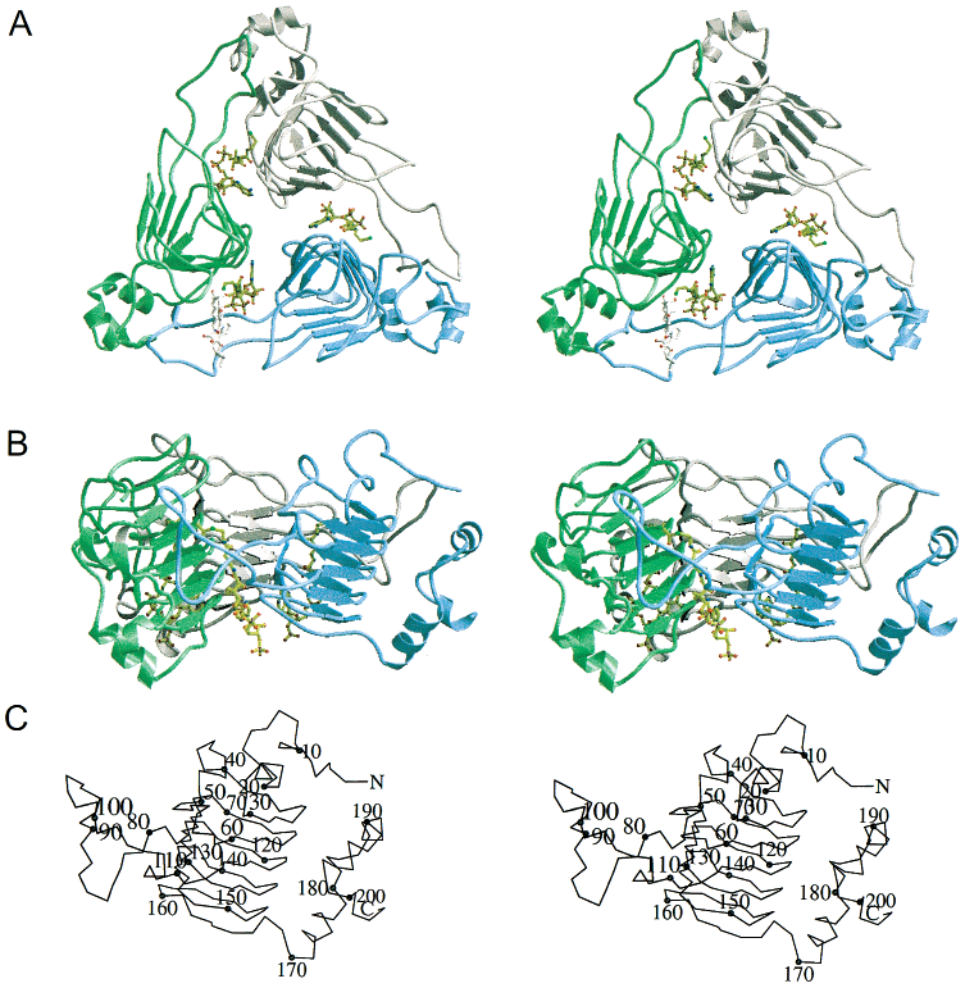

FIGURE 3: Overall structure of Vat(D) complexes. (A) Vat(D)−virginiamycin M_1−CoA complex viewed parallel to the crystallographic 3-fold axis that relates subunits of the trimer, depicting three CoA molecules and one molecule of virginiamycin M_1. (B) Vat(D)−acetyl-CoA complex viewed nearly perpendicular to the 3-fold axis. The A subunit mentioned in the text is shown on the left (green), and the B subunit is on the right (blue) when viewed from this direction. (C) Polypeptide chain conformation of a Vat(D) subunit. The direction of the view is the same as that for the B (blue) subunit of panel B. This figure was prepared with Molscript (*35*) and Raster3D (*36*, *37*).

unit. However, significant density for the virginiamycin M_1 substrate was found in just three active sites, arranged as two active sites in one trimer and one active site in the remaining trimeric molecule. Data measurement, model building, and least-squares refinements for the complex structures were carried out in the same manner as for the apoenzyme form II structure determination while maintaining the same set of reflections for the calculation of R_{work} and R_{free}.

RESULTS AND DISCUSSION

Overall Structure of Vat(D). The structure of Vat(D) was determined from two orthorhombic crystal forms which appeared in crystallization trials from different protein preparations. The apoenzyme structure from the form I crystals was determined to 2.5 Å resolution and refined to an R_{factor} of 20.6% (R_{free} = 28.0%). The overall stereochemistry of the atomic model is good, with rms deviations from ideality for bond lengths and bond angles of 0.010 Å and 1.5°, respectively. Geometric analysis of the structure with Procheck (*33*) indicates that 87% of the main chain torsion angles are found in the most favored region of the Ramachandran plot, 13% are found in the additionally allowed region, and none is found in the generously or disallowed regions. The apoenzyme structure of the form II crystals was determined by molecular replacement using the newly determined form I coordinates. The rms deviation of the α-carbon coordinates of the form I and form II structures is 0.20 Å, indicating that these structures are nearly identical.

The enzyme is a homotrimer, with its subunits related by a noncrystallographic 3-fold axis in both crystal forms. The trimer has overall dimensions of ∼76 Å × 76 Å × 35 Å, with the shortest dimension parallel to the noncrystallographic 3-fold axis (Figure 3). The overall structure of the Vat(D) subunit is folded into three domains: a large coiled LβH structural domain, an extended loop domain that projects from the LβH domain, and a C-terminal domain. The 29 N-terminal residues form a cap of the LβH domain.

The largest structural domain of Vat(D) is the left-handed parallel β-helix (LβH) domain composed of five triangular coils (residues 30−156) wound in the form of a triangular prism (*15*). This domain corresponds to a series of imperfect tandem-repeated sequences described as [LIV]-[GAED]-X_2-[STAV]-X and termed hexapeptide repeats (*13*, *14*). The triangular coils are formed by three short β-strands and turns, termed PB1, PB2, and PB3 and T1, T2, and T3 (Figure 4).

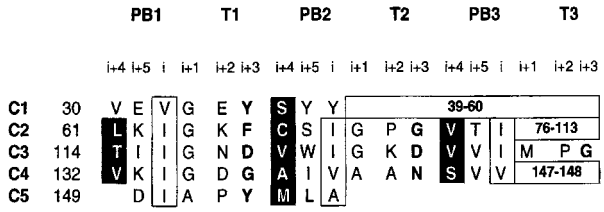

FIGURE 4: Structure-based amino acid sequence alignment of the LβH domain of Vat(D) (residues 30−156) identifying structurally equivalent residues in each of the five coils. Each horizontal line represents one complete or partial coil. The parallel β-strands that form the planar faces of the LβH are denoted PB1, PB2, and PB3, and the turns separating these strands are denoted T1, T2, and T3. The residue types within each hexapeptide unit are indicated (*i*, *i* + 1, ...). The conserved hydrophobic residues at position *i* are boxed. Residues in the left-handed conformation (positive main chain torsion angle φ) at position $i + 3$ are depicted in bold type. The small residues at the corners of each coil at position $i + 4$ are reverse shaded. Residues not involved in the coiled β-helical structure are enclosed in boxes and include an extrahelical loop (residues 39−60) and the longer extended loop domain formed by residues 76−113, both contributed from turn T3.

A single β-strand and turn correspond to one hexapeptide repeat unit. Hydrogen bonding between adjacent coils forms the faces of the LβH domain, which are extremely flat parallel β-sheets. The imperfect hexapeptide repeat sequence motif is characterized by the occurrence of aliphatic residues (Leu, Ile, or Val) at position *i*, a small residue (typically Ser, Thr, Ala, or Val) at position $i + 4$ which projects into the lumen of the LβH domain, and often a Gly residue at position $i + 1$. The three LβH domains lean away from the 3-fold axis, forming a 23° angle with this axis.

The regular coiled conformation of the LβH domain is interrupted at two locations by external loops. The first such loop contains residues 39−60. The second is a longer extended loop domain composed of residues 76−113 which donates most of the residues that interact with the antibiotic. Neither external loop obeys the hexapeptide repeat sequence rule of the LβH domain. As a result, these loops project outward from the LβH domain from the same T3 turn positions of successive triangular coils and re-enter the LβH fold at the same positions. An N-terminal cap (residues 1−29) rests against the top face of the LβH domain. A C-terminal domain, consisting of four α-helices (residues 170−179, 186−189, 193−197, and 201−205), forms intersubunit contacts with the extended loop domain of an adjacent subunit.

Superposition of the α-carbon atomic coordinates of residues 59−160 of Vat(D) (corresponding to the LβH domain) onto the α-carbons of residues 55−157 of PaXAT (1XAT) yields an rms deviation of 1.3 Å. The differences in the overall structures of these two enzymes can largely be attributed to the two external loops and the 29 N-terminal residues.

Active Site of Vat(D). The structures of two Vat(D) complexes were determined by molecular replacement using native form II crystals that had been soaked in solutions containing either acetyl-CoA or virginiamycin M_1 and CoA and determined to resolutions of 2.7 and 2.8 Å, respectively. The main chain conformations of the apoenzyme and complex structures are all nearly identical with rms deviations of 0.19 Å between α-carbon coordinates, indicating that little main chain conformational change has taken place upon binding of the substrates.

The active site of Vat(D) is marked by the binding site for the cofactor and is formed at the interface between two adjacent subunits of the trimeric enzyme, termed A and B (Figure 3B). Each trimeric molecule contains three such active sites. The asymmetric unit of the form II crystals contains two trimeric molecules, and each of the six active sites binds CoA. The substrates bind at opposite ends of a tunnel. This tunnel is formed by three small residues at the $i + 1$ position of three adjacent coils of the LβH domain of subunit A (Gly 70A, Gly 123A, and Ala 142A) and residues from the LβH and extended loop domains of subunit B. The solvent accessibility of CoA is reduced by 81% on binding to the enzyme.

The binding conformation of both CoA and acetyl-CoA is characterized by an overall bent conformation of the cofactor, a solvent-shielded pantetheine arm adopting an extended conformation directed parallel to the subunit−subunit interface, a 3′ solvent-exposed phosphate, and the cofactor adenine ring pointing toward the protein in an *anti* glycosidic linkage. Two of the pyrophosphoryl oxygens of the cofactor interact directly with Lys 111B and more distantly with Lys 165A and Lys 148B. The adenine ring exocyclic amino group is within hydrogen bonding distance of an active site water molecule, while the carbonyl oxygen atoms of the extended pantetheine arm hydrogen bond to the peptide nitrogen atoms of Lys 124A and Ala 142A, two residues that stack on top of one another at identical $i + 2$ positions of coils C3 and C4. These carbonyl oxygens are separated by 5.0 Å, corresponding to a distance of 4.9 Å between adjacent β-strands of the coiled LβH domain. The hydrogen bonds to the rigidly spaced coils of the LβH domain account for the extended conformation of the cofactor pantetheine arm and direct it toward the substrate acceptor binding pocket. His 82B projects from the extended loop domain where its imidazole NE2 atom is within hydrogen bonding distance of the thiol group of CoA. The ND1 atom of this residue donates a hydrogen bond to the peptide oxygen of Thr 88B, stabilizing a tautomeric form of the imidazole for which this atom is protonated. The imidazole ring of His 82B stacks against Trp 121A of the opposite subunit (Figure 5C). The conformation of acetyl-CoA bound to Vat(D) is similar to that of CoA. The acetyl group carbonyl oxygen appears to accept a hydrogen bond from the indole NE1 atom of Trp 121A.

Virginiamycin M_1 binds to two active sites in one trimer and to just one active site in the remaining trimeric molecule. The reason for the apparent differences in binding occupancy of the six active sites in the asymmetric unit of these crystals is not known, and does not appear to correlate with any significant conformational differences of the enzyme. The antibiotic binding pocket is located primarily in the B subunit and results in a reduction of 79% in the solvent accessibility of the drug on binding to the enzyme. The overall conformation of the enzyme-bound virginiamycin M_1 molecule differs significantly from the small molecule structure of the antibiotic, placing the dehydroproline group over the lumen of the macrolactone ring and in contact with the dienyl amide portion of the molecule (Figure 5A).

The contacts to the antibiotic are donated predominantly by the two external loops that are excluded from the LβH

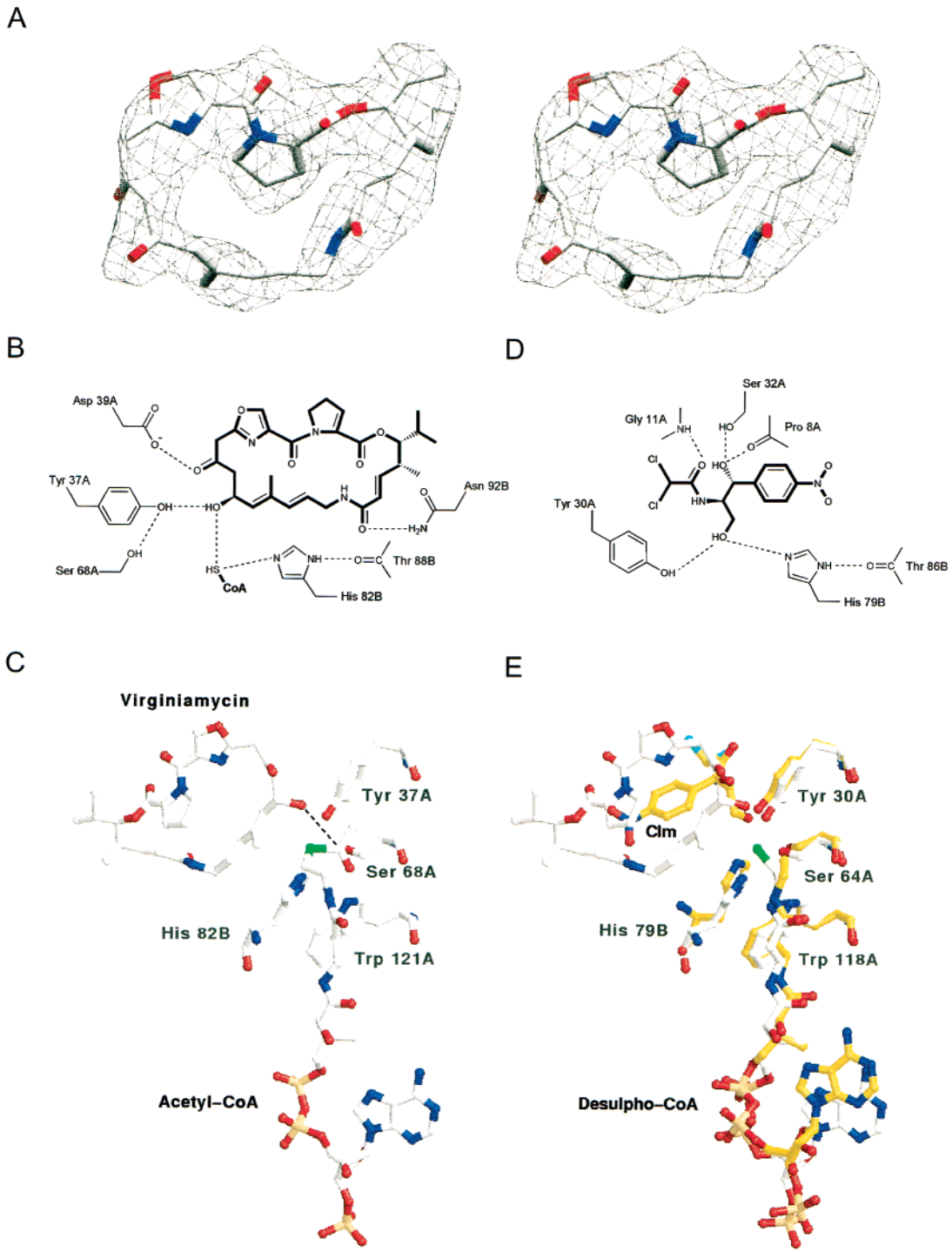

FIGURE 5: Active site of Vat(D). (A) Stereoview of a priori unbiased $F_o - F_o$ electron density corresponding to virginiamycin M_1 contoured at 1.5σ. (B) Schematic diagram depicting the hydrophilic interactions at the active site of the Vat(D) virginiamycin M_1−CoA complex. (C) The active site of Vat(D) derived from the superposition of acetyl-CoA coordinates onto those of the virginiamycin M_1−CoA complex. Residues from the A and B subunits are depicted as are the substrate virginiamycin M_1 and cofactor acetyl-CoA. The dotted line joins the attacking hydroxyl group of the antibiotic and the carbonyl carbon atom of the thioester. The labels refer to the Vat(D) structure. (D) Schematic diagram depicting the hydrophilic interactions at the active site of the PaXAT Clm−desulfo-CoA complex. (E) Superposition of the active sites of the Vat(D) virginiamycin M_1−CoA complex (white bonds) with the PaXAT Clm−desulfo-CoA complex (yellow bonds). The labels refer to the PaXAT structure. This figure was prepared with Molscript (*35*), Raster3D (*36*, *37*), and Setor (*38*).

domain (residues 39−60 or extended loop residues 76−113). These include hydrophobic contacts with Tyr 54B, Leu 93B, Pro 103B, Leu 108B, and Val 17A as well as hydrogen bonds of the side chain groups of Asp 39A and Asn 92B with carbonyl groups of the antibiotic (Figure 5B). The modified hydroxyl of the antibiotic hydrogen bonds to the phenolic hydroxyl of Tyr 37A and is within 3.1 Å of the sulfhydryl group of CoA and 4.4 Å from the NE2 atom of His 82B.

A superposition of the acetyl-CoA coordinates onto the structure of the virginiamycin M_1−CoA ternary complex structure places the antibiotic hydroxyl group within 3.3 Å of the acetyl group carbonyl carbon and suggests that this

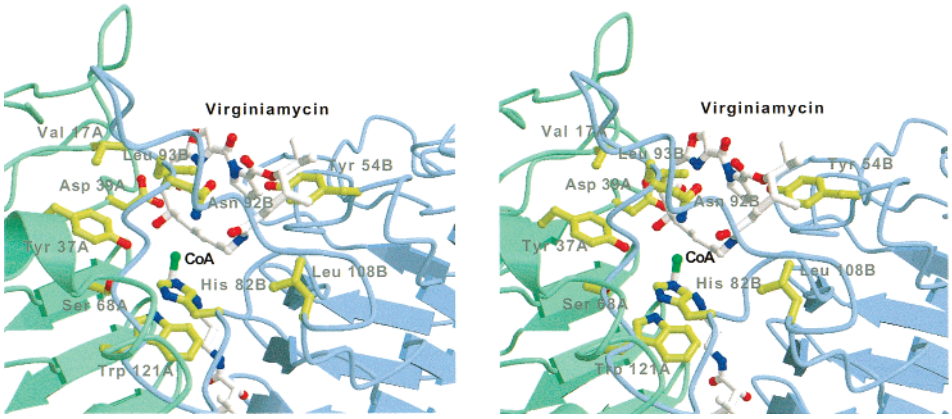

FIGURE 6: Vat(D) in complex with CoA and virginiamycin M_1. The direction of view is similar to that in Figure 3B, and depicts the A subunit (green) and B subunit (blue) contributing to the active site. The extended loop (residues 76−113) is visible. This figure was prepared with Molscript (*35*) and Raster3D (*36*, *37*).

hydroxyl could be in position for direct attack (Figure 5C). His 82B donates a hydrogen bond from its ND1 group to the main chain carbonyl oxygen of Thr 88B and participates in a ring stacking interaction with Trp 121A. Both of these interactions would be expected to increase its basicity and to facilitate a proposed role as a general base, although a conformational change of the enzyme or repositioning of the antibiotic would be required to bring the NE2 group and the antibiotic hydroxyl group close enough for proton abstraction.

A similar active site location and pattern of interactions of a histidine residue is observed in all hexapeptide acyltransferases for which detailed active site information is known, including PaXAT (see below) and *Escherichia coli* GlmU, a bifunctional hexapeptide acetyltransferase that catalyzes acetylation of GlcN-1-PO_4 prior to the condensation of the acetylated product with UTP to form UDP-GlcNAc and pyrophosphate (*20*−*22*). GlmU His 363A is positioned at the acetyltransferase active site in a binary complex of the enzyme with CoA (His 363A NE2−CoA sulfur distance of 6.0 Å). Similarly, its imidazole ring stacks against the aromatic ring of Tyr 366B, while its ND1 group interacts with the side chain of Glu 349B. This general pattern of interactions may be catalytically important since they are observed in Vat(D), GlmU, and PaXAT, even though His 363A of GlmU is donated from the opposite (A) subunit to His 82B of Vat(D).

The virginiamycin antibiotic hydroxyl group also hydrogen bonds to the phenolic hydroxyl of Tyr 37A. The role of this residue is uncertain, but it could serve to position the attacking hydroxyl group of the antibiotic or otherwise facilitate its attack on the thioester. The catalytic properties of Vat(D) and its interactions with virginiamycin M_1 described here may be shared with the structurally similar dalfopristin semisynthetic component of Synercid, which is also a substrate for Vat(D) (*5*).

Comparison to the CATB Acetyltransferases. Superposition of the α-carbon coordinates corresponding to the LβH domain of Vat(D) with PaXAT yields an rms discrepancy of 1.3 Å for atoms of the LβH domain. The overall polypeptide chain fold of these enzymes is very similar, with the greatest dissimilarities in the N-terminal domain and two loops that project from the LβH domain. The key active site residues of Vat(D) are conserved in PaXAT, and include Tyr 37A, His 82B, and Trp 121B [Vat(D) numbering; Figure 5D,E]. This structural alignment also superimposes the modified hydroxyl groups of virginiamycin M_1 and Clm within 1.3 Å, the NE2 atoms of the active site histidine residues within 1.2 Å, and the hydroxyl groups of the active site tyrosine residues within 0.9 Å of one another, demonstrating that the CATB and Vat acetyltransferases share geometrically similar active sites and probably very similar chemical mechanisms.

Although the covalent structures of virginiamycin M_1 and Clm are very different (Figure 1), some aspects of their structures are recognized in a similar manner (Figures 5B,C and 6). Two equivalent residues, Phe 91B of PaXAT and Leu 93B of Vat(D), interact with the *p*-nitrophenyl group of Clm and hydrophobic groups of the virginiamycin M_1 macrocyclic ring, respectively. Ser 32A of PaXAT and Asp 39A of Vat(D) are also equivalent and interact with the unmodified secondary hydroxyl of Clm and a virginiamycin M_1 carbonyl oxygen. These shared substrate recognition features may also be utilized by CATB enzymes as they interact with their natural substrate(s).

Despite the overall similarities in the polypeptide chain fold and active site geometry, the substrate specificities of Vat(D) and PaXAT do not overlap. The CATB acetyltransferases are not known to modify any substrate other than Clm (*3*). Conversely, for Vat(D), we measured K_m values for virginiamycin M_1 and acetyl-CoA of 26 ± 2.8 and 303 ± 58 μM, respectively, with an apparent V_{max} for the reaction of 564 ± 18 μmol min^{-1} mg^{-1}, but could not detect activity against Clm at concentrations of up to 0.1 M. This substrate specificity can be rationalized from the atomic models of the two enzymes. The position of virginiamycin M_1 superimposed in the active site of PaXAT creates numerous steric conflicts with the enzyme. Among the structural features that would prevent binding of Clm to Vat(D) are steric conflicts with Leu 93B and Phe 94B and the lack of any significant hydrophobic interaction of the nitrophenyl ring with residues of Vat(D) as occurs with PaXAT Phe 9A.

The development of additional streptogramin-based antibiotics may be necessary to keep apace of drug resistant microorganisms such as cocci of the *vat* genotype whose evolution and dissemination have been promoted by the overuse of virginiamycin as a livestock growth promoter. The Vat-mediated cross resistance of these organisms to the dalfopristin component of Synercid used in human therapy

is cause for concern that such resistance to a last resort antibiotic could be transferred with increasing frequency to human pathogens. An understanding at the atomic level of the mechanisms that confer resistance to streptogramin antibiotics, such as the Vat-mediated acetylation of the group A component of streptogramins, may direct the search for antibiotics that evade the action of these enzymes or inhibit their activity.

ACKNOWLEDGMENT

We gratefully acknowledge the assistance of Drs. Todd Beaman, Larry Olsen, and Wuxian Shi and helpful discussions with Dr. John S. Blanchard.

REFERENCES

1. Roberts, M. C., Sutcliffe, J., Courvalin, P., Jensen, L. B., Rood, J., and Seppala, H. (1999) *Antimicrob. Agents Chemother. 43*, 2823−2830.
2. Bunny, K. L., Hall, R. M., and Stokes, H. W. (1995) *Antimicrob. Agents Chemother. 39*, 686−693.
3. White, P. A., Stokes, H. W., Bunny, K. L., and Hall, R. M. (1999) *FEMS Microbiol. Lett. 175*, 27−35.
4. Barriere, J. C., Berthaud, N., Beyer, D., Dutka-Malen, S., Paris, J. M., and Desnottes, J. F. (1998) *Curr. Pharm. Des. 4*, 155−180.
5. Rende-Fouriner, R., Leclercq, R., Galimand, M., Duval, J., and Courvalin, P. (1993) *Antimicrob. Agents Chemother. 37*, 2119−2125.
6. Allignet, J., Liassine, N., and El Solh, N. (1998) *Antimicrob. Agents Chemother. 42*, 1794−1798.
7. Allignet, J., and El Solh, N. (1995) *Antimicrob. Agents Chemother. 39*, 2027−2036.
8. Jensen, L. B., Hammerum, A. M., Aarestrup, F. M., van den Bogaard, A. E., and Stobberingh, E. E. (1998) *Antimicrob. Agents Chemother. 42*, 3330−3331.
9. Allignet, J., Loncle, V., Simenel, C., Delepierre, M., and El Solh, N. (1993) *Gene 130*, 91−98.
10. Bozdogan, B., and Leclercq, R. (1999) *Antimicrob. Agents Chemother. 43*, 2720−2725.
11. Mukhtar, T., Koteva, K., Hughes, D., and Wright, G. (2001) *Biochemistry 40*, 8877−8886.
12. Vannuffel, P., and Cocito, C. (1996) *Drugs 51* (Suppl. 1), 20−30.
13. Vaara, M. (1992) *FEMS Microbiol. Lett. 97*, 249−254.
14. Dicker, I. B., and Seetharam, S. (1992) *Mol. Microbiol. 6*, 817−823.
15. Raetz, C. R. H., and Roderick, S. L. (1995) *Science 270*, 997−1000.
16. Kisker, C., Schindelin, H., Alber, B. E., Ferry, J. G., and Rees, D. C. (1996) *EMBO J. 15*, 2323−2330.
17. Beaman, T. W., Binder, D. A., Blanchard, J. S., and Roderick, S. L. (1997) *Biochemistry 36*, 489−494.
18. Beaman, T. W., Sugantino, M., and Roderick, S. L. (1998) *Biochemistry 37*, 6689−6696.
19. Brown, K., Pompeo, F., Dixon, S., Mengin-Lecreulx, D., Cambillau, C., and Bourne, Y. (1999) *EMBO J. 18*, 4096−4107.
20. Kostrewa, D., D'Arcy, A., Takacs, B., and Kamber, M. (2001) *J. Mol. Biol. 305*, 279−289.
21. Olsen, L. R., and Roderick, S. L. (2001) *Biochemistry 40*, 1913−1921.
22. Sulzenbacher, G., Gal, L., Peneff, C., Fassy, F., and Bourne, Y. (2001) *J. Biol. Chem. 276*, 11844−11851.
23. Murray, I. A., and Shaw, W. V. (1997) *Antimicrob. Agents Chemother. 41*, 1−6.
24. Shaw, W. V. (1983) *CRC Crit. Rev. Biochem. 14* (1), 1−46.
25. Cleland, W. W. (1979) *Methods Enzymol. 79*, 103−188.
26. Sugantino, M., and Roderick, S. L. (2000) *Acta Crystallogr. D56*, 640−642.
27. Kabsch, W. (1988) *J. Appl. Crystallogr. 21*, 916−924.
28. Otwinoski, Z., and Minor, W. (1997) in *Methods in Enzymology* (Carter, C. W., Jr., and Sweet, R. M., Eds.) pp 307−326, Academic Press, New York.
29. Brunger, A. T., Krukowski, A., and Erickson, J. W. (1990) *Acta Crystallogr. A46*, 585−593.
30. Jones, T. A., Zou, J.-Y., Cowan, S. W., and Kjeldgaard, M. (1991) *Acta Crystallogr. A47*, 110−119.
31. Brunger, A. T. (1992) *Nature 355*, 472−475.
32. Navaza, J. (1994) *Acta Crystallogr. D50*, 157−163.
33. Laskowski, R. A., MacArthur, M. W., Moss, S. D., and Thornton, J. M. (1993) *J. Appl. Crystallogr. 26*, 283−291.
34. Barton, G. J. (1993) *Protein Eng. 6*, 37−40.
35. Kraulis, P. J. (1991) *J. Appl. Crystallogr. 24*, 946−950.
36. Merrit, E. A., and Murphy, M. E. P. (1994) *Acta Crystallogr. D50*, 869−873.
37. Bacon, D. J., and Anderson, W. F. (1996) *J. Mol. Graphics 6*, 219−220.
38. Evans, S. V. (1993) *J. Mol. Graphics 11*, 134−138.

BI011991B